



Experimental Assessment of the Power Conversion of a Wave Energy Converter Using Hydraulic Power Take-Off Mechanism

Tri Dung Dang^{1,3} · Tri Cuong Do² · Kyoung Kwan Ahn¹

Received: 12 February 2020 / Revised: 21 July 2020 / Accepted: 25 August 2020 / Published online: 29 October 2020
© Korean Society for Precision Engineering 2020

Abstract

The hydraulic power take-off (HPTO) is considered as the most promising method to convert wave power to electrical power. This paper presents an experimental assessment of the power conversion of a wave energy converter using HPTO. Based on the experimental results, a modification of accumulator pre-charged pressure and a control strategy were proposed to improve the system performance. System design, the working principle and mathematical model of all components were described. The proposed method was verified based on both simulation and experimental tests. The results showed that the system always works at an optimal condition under different input wave conditions.

Keywords Wave energy converter · Hydraulic power take-off · Modeling · Experiment · Motors · Cylinders

1 Introduction

Electricity production by clean, safe and sustainable energy sources is nowadays a priority for many industrialized countries due to increasing energy demand and reducing CO₂ emissions. Wind, solar and wave energy have become great candidates to provide the solution for a long time. Among them, wave energy shows considerable technical advantages compared to wind and solar. It is not only a substantial clean energy supply but also more predictable, persistent and spatially concentrated [1]. As stated by Johannes Falnes [1], the power flow intensity of solar and wind energy can be up to 2–3 kW/m² as they are converted to wave energy. This increase in power intensity and the fact that wave energy is more persistent than the others stimulate motivation for developing wave power technology to a prosperous mature level in the future. Although being underestimated as no commercialized products are available in the market [2–4],

still wave energy is a fresh, promising approach for a solution to the greenhouse gases (GHG) emission problem.

There are hundreds of concepts for WEC technologies [2–4] but only a few full-scale devices have been investigated in real sea conditions. Based on WEC development [4], the point absorber type has received more attention, because it is the simplest and cheapest type. Their diameters are significantly smaller than the wavelength, and the point absorbers can harvest wave energy in all directions. There is a large number of existing works using point absorber. Reacting to the wave motion, the buoy is forced to move up and down. Then, these movements can be transmitted to drive a translational motion of the linear generator [5]. This type of power take-off (PTO) has faced several challenges such as the linear generator is still in a premature stage, the system size strongly depends on the rated force of the WEC device and the wave conditions [6].

Another type is mechanical PTO WEC. The advantage of this type is that the rotary generator can be used since a mechanical transmission i.e. rack-and-pinion and gearbox can convert the translational motion of the wave to rotational motion [7–11]. Some previous studies also showed that some subsystems can be applied to improve system performance. Inertia [8], stiffness [9] and output speed [11] of the system can be controlled using some extra mechanisms to achieve higher efficiency. One drawback of this type is necessary for frequent maintenance due to a large number of short-lifetime-moving parts [6].

✉ Kyoung Kwan Ahn
kkahn@ulsan.ac.kr

¹ Department of Mechanical Engineering, University of Ulsan, Nam-gu, Ulsan 44610, Korea

² Graduate School of Mechanical Engineering, University of Ulsan, Nam-gu, Ulsan 44610, Korea

³ Department of Mechatronics, Ho Chi Minh City University of Technology and Education, Ho Chi Minh City 700000, Vietnam

The use of hydraulics PTO is the most appropriate method for WEC due to its particular suitability for the movements of wave devices, the pitching of a lever arm or the vertical motion of a buoy against a stationary reference can easily be used to drive a piston in a pump or a hydraulic ram. The transmission efficiency can reach 90% [6]. Besides, hydraulic components are available from commercial manufacturers. Another advantage is the ease of incorporating energy storage, which can be done using a high-pressure accumulator or a set of high-pressure/low-pressure accumulators. Most of these existing technologies have shown good concepts along with working principles [12–17]. However, the energy conversion efficiencies are limited by many factors such as loss for friction or viscous, improper working conditions of equipment, etc. Some researchers have proposed methods to increase the output power of hydraulic PTO WEC. Do et al. [18, 19] and Tri et al. [20] found the influence of the sliding angle of the buoy comparing to the vertical direction to the power performance and proposed their methods to achieve the optimal slope. Another method was presented in [21] where they stabilized the output power using the pressure coupling principle. Ahn [22] and Truong [23] proposed a combination of mechanical-hydraulic PTO to exploit the advantages of both types. The concept is promising but it lacks experimental results. As investigated by Cargo [24–26], the component that contributes to the main power loss in the circuit is the hydraulic motor, whose loss is up to 40% of the loss in the hydraulic circuit. The motor has an optimum working condition relating to the ratio between speed and pressure. It is important to set the motor to work in a high-efficiency working range. In this way, the loss caused by the hydraulic motor can be reduced. Consequently, system performance and efficiency will be increased.

The goal of this paper is to investigate an experimental case study of a hydraulic PTO and propose a control strategy to improve system performance. First, the PTO mechanism was described. Then, a numerical model of the floating buoy system was presented to investigate the performance of the system under ocean waves. The hydrodynamic behavior of the floating buoy was analyzed by linear potential wave theory and simulation was performed in Matlab/Simulink environment. These results were sent to control the test rig. Finally, the control strategy was presented and verified through both simulation and experiment.

2 System Configuration, the Working Principle and Test Rig

The hydraulic PTO WEC typically consists of the hydraulic cylinders, rectifier valves (control manifold), the hydraulic motor, the accumulators, the safety valves and the connecting hoses. A rotary generator driven by the

hydraulic circuit is then employed to produce electricity. In a full-scale system, several hydraulic cylinders are connected to a single hydraulic circuit (multi-float system) to take advantage of the hydraulic transmission and to reduce the system cost. Based on this configuration, the structure of an experimental test rig is shown in Fig. 1. As given, the proposed system can be divided into two parts: a wave–buoy simulator and an energy recovery system.

The wave–buoy interaction simulator contains five bottom cylinders and a hydraulic power pack that has an electric motor driving a hydraulic pump. The power pack supplies hydraulic fluid to five bottom cylinders through five proportional valves. The bottom cylinders represent the buoy motion under the wave. To mimic the real conditions, wave frequencies and amplitudes were calculated based on the hydrodynamic model of ocean wave and a floating buoy. Then, the wave profile and wave forces were used as the reference to control each cylinder. The velocity and position of the cylinder were separately controlled by PID controllers to achieve the wave motion. A relief valve (RLV3) was placed at the outlet port of the hydraulic pump. The force of the cylinder depends on the pressure of the system. Therefore, by using the relief valve, the pressure in the circuit and the force of the cylinder can be adjusted respect to the different wave conditions in the ocean.

The energy recovery system includes five upper cylinders, check valves, a high-pressure accumulator (HPA), a hydraulic motor, a hydraulic pump and a relief valve. By coupling each pair of top and bottom cylinders, the motions of five upper cylinders are also driven to follow the wave motions. The five upper cylinders convert the wave energy from mechanical power into hydraulic power. The pair of check valves were placed in opposite directions allow the hydraulic fluid in the bore chamber is pressed to high-pressure and go to the high-pressure hydraulic circuit when these cylinders go up and pump oil fluid from tank return to the bore chamber when they move down. During the moving up process, one part of the flow is used to drive the hydraulic motor and the excess is stored in the (HPA). The HPA keeps the operating pressure constant, then the speed of the hydraulic motor is stabilized. In the test rig, we used a hydraulic pump and a relief valve coupled with the hydraulic motor to simulate the load of the generator instead of a real generator. The resistive load causes by the pump can be adjusted by adjusting the set pressure of the relief valve (RLV2). A relief valve (RLV1) was also installed for safety. Some sensors such as load cell, pressure sensors and flow sensors are installed to monitor the current states of the WEC system.

The experimental setup was built to verify the performance of the proposed control strategy for the WEC system. A test rig was assembled as shown in Fig. 2. The total system includes the main parts as described above. The parameters

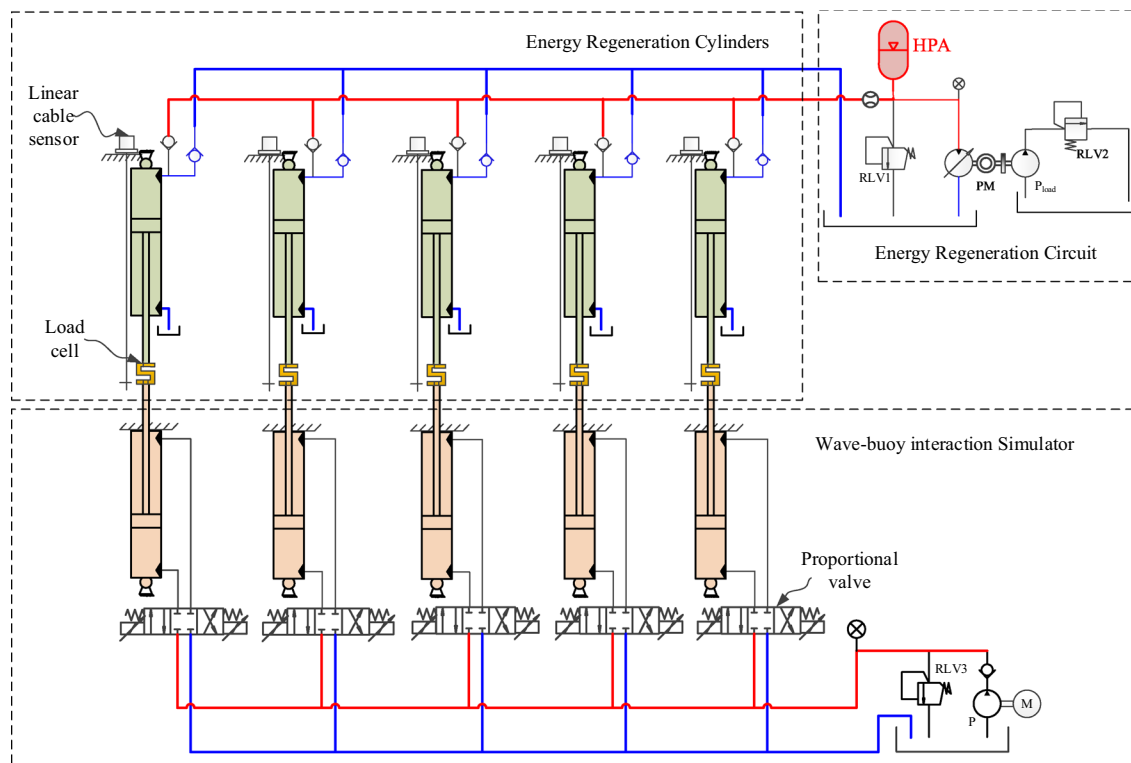


Fig. 1 Schematic diagram of the WEC system

of the experimental system are shown in Table 1. System parameters were chosen so that it can produce up to 5 kW output power based on the wave data of some offshore sites in South Korea [27].

3 Wave—Buoy Interaction Model, Hydraulic System Model

3.1 Wave—Buoy Interaction Model

Figure 3 shows the schematic diagram of the wave and buoy interaction of a WEC using a floating buoy coupled with a hydraulic power take-off cylinder. The hydrodynamic force acting on the floating buoy such as excitation force, radiation force, hydrostatic force and reactive force from the PTO system [28] defines the motion of the float. The buoy motion under the wave elevation is denoted as z . The hydrodynamic equation of buoy motion is obtained by Newton’s second law:

$$M_b \ddot{z} = F_H - F_{PTO} \tag{1}$$

where M_b is the buoy mass, F_H is the hydrodynamic force and F_{PTO} is the resistive force from the cylinder.

The hydrodynamic force, which is the sum of the excitation force F_e , the radiation force F_r , and the hydrostatic force F_{hs} , is calculated by:

$$F_H = F_e + F_r + F_{hs} \tag{2}$$

where

$$F_e = f_e(\omega)Y(\omega) \tag{3a}$$

$$F_r = -m_r(\omega)\ddot{z} - R_r(\omega)\dot{z} \tag{3b}$$

$$F_{hs} = \rho g V_b \tag{3c}$$

There are some hydrodynamic coefficients defined by: f_e is the excitation force coefficient, Y is the wave amplitude; m_r is the added masses, R_r is the radiation damping coefficient; where ρ is the water density, g is the gravitational acceleration and V_b is the submerged volume of the buoy.

These hydrodynamic coefficients can be calculated by using the WAMIT commercial software (version 7.0) [29].

The resistive force is computed by:

$$F_{PTO} = P_{bore} A_{bore} \tag{4}$$

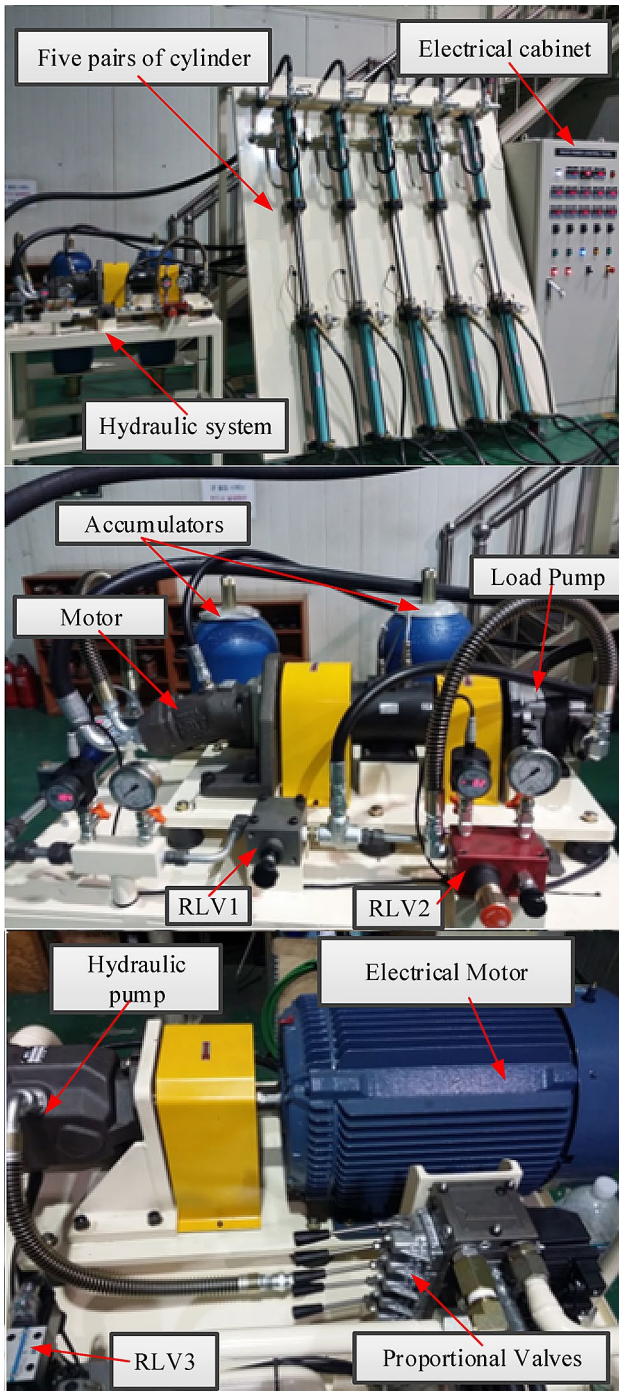


Fig. 2 Experimental setup for the WEC system

where P_{bore} and A_{bore} are the pressure of fluid inside the cylinder bore chamber and area of bore chamber, respectively.

3.2 Hydraulic System Mathematical Model

Five cylinders work as a hydraulic pump to convert wave energy into hydraulic energy of the fluid flow. The

Table 1 Parameters of the simulation model and system specification

Components	Capacity	Unit
Cylinder		
Piston diameter	40	[mm]
Rod diameter	20	[mm]
Length	0.45	[m]
Max pressure	130	[bar]
HPAs		
Volume	20	[L]
Gas pre-charged pressure	70 and 110	[bar]
Max pressure	250	[bar]
Hydraulic motor		
Displacement	28	[cc/rev]

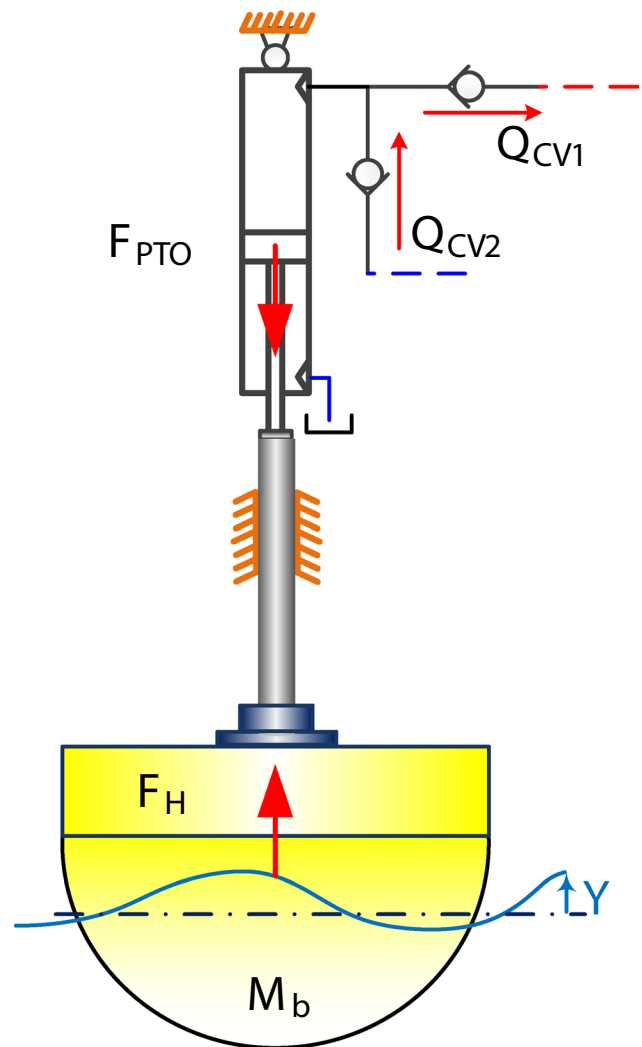


Fig. 3 Wave and buoy interaction of the floating buoy in WEC

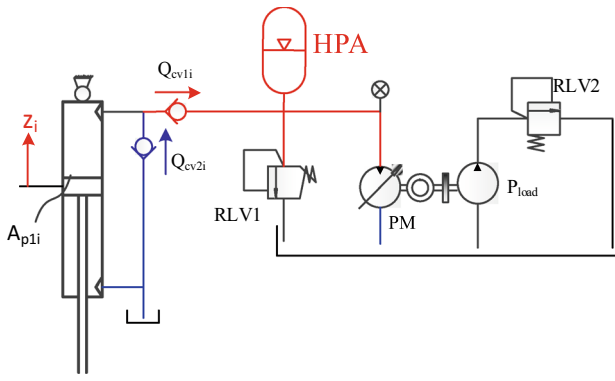


Fig. 4 Hydraulic power take-off system

hydraulic diagram of one cylinder and the hydraulic circuit is shown in Fig. 4. Consider the i th cylinder, with i from 1 to 5, the pressure inside the bore chamber is denoted by P_i , which can be calculated using this equation:

$$\frac{dP_i}{dt} = \frac{\beta}{V_{0i} + A_c(-z_i)} (A_c \dot{z}_i - Q_{cv1i} + Q_{cv2i}) \quad (5)$$

where β is the bulk modulus of fluid; A_c is the piston area in the bore chamber; V_{0i} is the initial volume, Q_{cv1i} and Q_{cv2i} are the flow rates through the check valve 1 and check valve 2, respectively. The flow rates are obtained by:

$$\begin{cases} Q_{cv1i} = C_d A_{o1} \sqrt{\frac{2(P_i - P_m)}{\rho_f}} & \text{if } P_i > P_m \\ Q_{cv1i} = 0, & \text{if } P_i \leq P_m \end{cases} \quad (6)$$

$$\begin{cases} Q_{cv2i} = C_d A_{o2} \sqrt{\frac{2(P_t - P_i)}{\rho_f}} & \text{if } P_t > P_i \\ Q_{cv2i} = 0, & \text{if } P_t \leq P_i \end{cases} \quad (7)$$

where C_d is the discharge coefficient, A_{o1} and A_{o2} are the working area of each check valve, ρ_f is the fluid density, P_t is the pressure of the fluid inside the tank, and P_m is the pressure in the main hydraulic line connected to high-pressure accumulator and can be obtained by the continuity equation:

$$\frac{dP_m}{dt} = \frac{\beta}{V_p + V_{hpa}} \left(\sum_{i=1}^5 Q_{cv1i} - Q_{hpa} - Q_m - Q_r \right) \quad (8)$$

where Q_m , Q_{hpa} and Q_r are the flow rates through the hydraulic motor, into the HPA and through the relief valve RLV1, respectively; V_p is the volume of the fluid inside the segmented pipe which connects the check valve 1 and the port in of the motor, and V_{hpa} is the entered fluid volume in the accumulator.

The flow rate Q_{hpa} and fluid volume V_{hpa} which enters the accumulator are calculated using:

$$V_{hpa} = \begin{cases} 0, & \text{if } P_m \leq P_0 \\ V_0 \left[1 - \left(\frac{P_0}{P_m} \right)^{\frac{1}{n}} \right], & \text{if } P_m > P_0 \end{cases} \quad (9)$$

$$Q_{hpa} = \dot{V}_{hpa} = \begin{cases} 0, & \text{if } P_m \leq P_0 \\ \frac{1}{n} V_0 \left(1 - \frac{P_0}{P_m} \right)^{\frac{1-n}{n}} \frac{P_0 \dot{P}_m}{P_m^2}, & \text{if } P_m > P_0 \end{cases} \quad (10)$$

where V_0 is the accumulator capacity, P_0 is the pre-charge pressure and n is the specific heat ratio.

The flow rate Q_r through the relief valve RLV1 is calculated as the following equation with p_{set} is the maximum safe pressure of the hydraulic system:

$$Q_r = \begin{cases} 0, & \text{if } P_m \leq p_{set} \\ C_d A_v \sqrt{2(P_m - P_t)/\rho}, & \text{if } P_m \geq p_{set} \end{cases} \quad (11)$$

And the flow rate via the motor is defined as:

$$Q_m = \frac{D\omega_m}{\eta_v} \quad (12)$$

where D is the motor displacement, ω_m is the motor angular speed, η_v is the volumetric efficiency.

The actual output torque of the motor is given as:

$$T_m = \eta_{tM} \Delta p D \quad (13)$$

$$T_m = J\dot{\omega}_m + C\omega_m + T_{load} \quad (14)$$

where Δp is the pressure difference between two ports of the motor, η_{tM} is the mechanical efficiency. J , C and T_{load} are respectively the motor inertial moment, viscous damping coefficient and the load rated torque created by the pump.

The total efficiency is obtained by multiplying mechanical and volumetric efficiency:

$$\eta_{tot} = \eta_{tM} \eta_v \quad (15)$$

4 Results and Discussion

4.1 Simulation and Experimental Progress

The progress of this study is shown in Fig. 5. The hydrodynamic parameters and coefficients were calculated by WAMIT software based on the wave and buoy parameters. Then using MATLAB/Simulink, we can obtain the wave

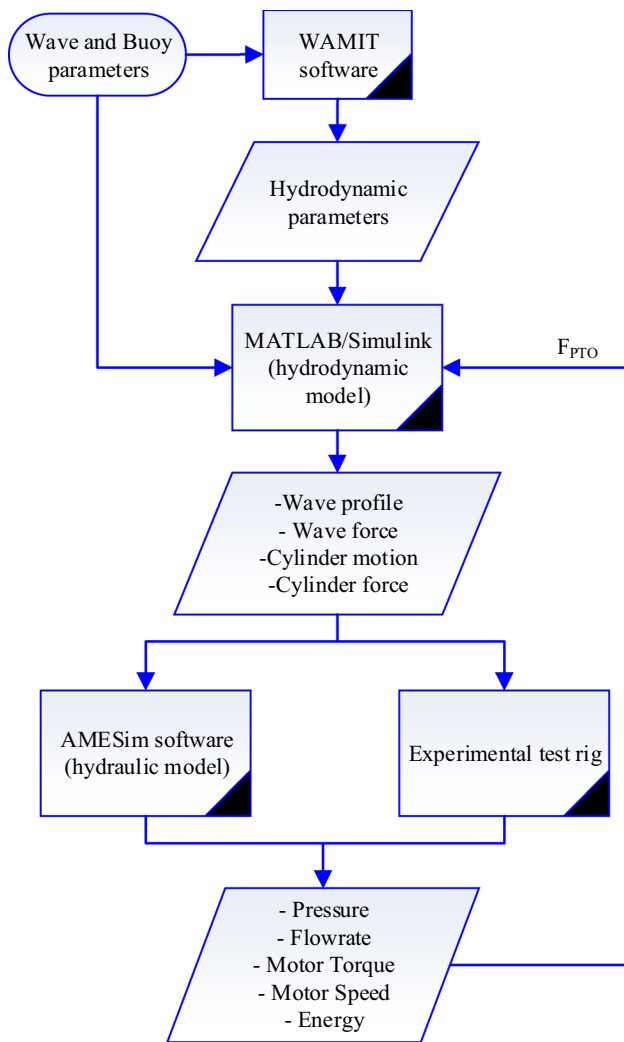


Fig. 5 Simulation flowchart to compute the buoy motion

profile, wave forces and hydrodynamic model which can describe the wave–buoy interaction of the WEC system. The information (cylinders motion and cylinders’ force) was then sent to the controller of the experimental test rig to achieve the mimic condition in the real environment. Consequently, the flow rate, system pressure, speed and torque of hydraulic motor as well as output energy and system efficiency can be obtained. As shown in the figure, the program will collect the resistive force of the PTO mechanism. This data will be used as input of the MATLAB/Simulink simulation program to compute the new value of the buoy/cylinder position at the next time step. The data were analyzed to obtain the efficiency map of the hydraulic motor. This map was embedded into the hydraulic circuit in the simulation model which was built in AMESim to easily apply control strategies and system modification. AMESim provides an environment to model fluid systems and control systems. It can help the user

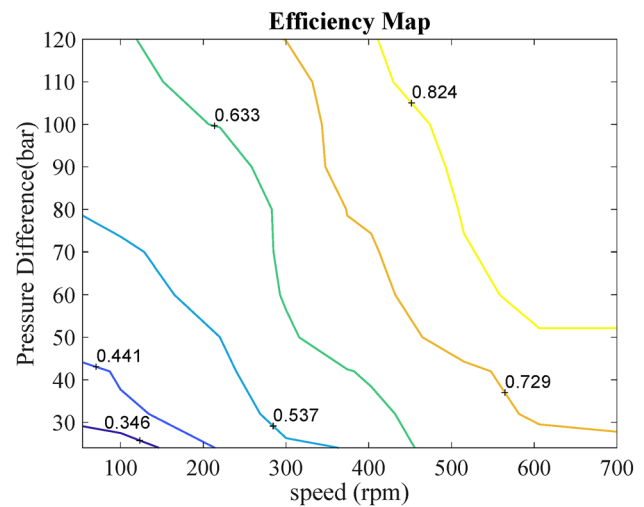


Fig. 6 Efficiency map of the hydraulic motor based on experimental results

investigate the dynamic behavior of hydraulic components and analyze the performance of specific components (e.g. hydraulic motor).

4.2 Motor Efficiency Map

As stated above, the motor contributes to the main power loss in the hydraulic system. In Eq. (12), the oil leakage is taken into account using the volumetric efficiency parameter, while mechanical friction and hydro-mechanical losses are taken into account using the mechanical efficiency in Eq. (13). It is true to say that motor efficiency depends on the rotational speed, the pressure difference between two ports of the motor. The relation between these parameters called a motor efficiency map that can be found by the manufacturer. However, if it is not available, we can obtain it using the experimental test. As shown in Fig. 6, the efficiency map of the hydraulic motor was built based on the experimental data. Torque and speed were measured under different experimental conditions with varying system pressure and flow rate by adjusting the wave conditions as in the simulation algorithm. Then the mechanical and volumetric efficiency map were derived based on Eqs. (12–13). The total efficiency was obtained by multiplying mechanical and volumetric efficiency. The map range is limited since the maximum working pressure of the hydraulic cylinder is 130 bar, and the threshold of the cylinder speed was also set lower than the bandwidth of the system. However, the map can still show the tendency and the optimal working range of the hydraulic motor. As

can be seen, bad selection in the working range can cause up to 70% loss in the hydraulic motor. Based on this, the next part of the paper will propose a control strategy to improve system performance.

4.3 Proposed Control Strategy

Based on the efficiency map of the hydraulic motor, it is important to drive it in the high-efficiency range. It should be noted that the pressure of the hydraulic motor depends on the wave force and the load conditions. While the speed of the hydraulic motor depends on the flow rate goes through it. The flow rate is a function of the cylinder motion since the piston's bore areas are constant.

The case in which the wave force is high is also the case that the cylinder moves with high amplitude (can be seen in Eqs. 3a and 5, also in Ref. [27]). In this case, the input wave power is high and flow rates from cylinders to the circuit are also high then we need to adjust the load at a high level to set the system working pressure as high level correspondingly.

In other cases, if the wave power is not high enough to produce a high force acting on the cylinders, we should maintain the flow rate at a high level to achieve high motor speed. It can also be done by adjusting the load at the medium or low level. If we set a high load level in this case, the reactive force of the system is too high that can prevent the cylinder motion thus reducing the flow rate.

Previous work [21] investigated and proved that the system performance is higher with the use of the hydraulic accumulator to prevent the fluctuation of the system pressure and flow rate. The pressure and flow rate vary from 0 to its peak values can reduce motor efficiency as seen in the map. In that work, we set two accumulators' pre-charged at 70 bar. In the case of high input power, the system pressure can reach 130 bar. The previous results showed that it took more than 20 s to charge the accumulator to reach a stable value. This lag time can cause a loss in the system. To reduce this, in this study we charged one accumulator to 110 bar to work in the high power condition and used the 70 bar accumulator to work in the medium power condition. If the input power produces a pressure lower than 70 bar, then no accumulator is used. In this case, only the load is controlled. The proposed control strategy is shown in Fig. 7.

4.4 Results and Discussion

To fully investigate the system performance and evaluate the effectiveness of the proposed control strategy, the WEC system hydraulic model was built in AMESIM v15.2 as shown in Fig. 8. We added two control valves to active one accumulator at a time depending on the input power condition. The cylinders were controlled as a sinusoidal profile with an amplitude of 0.2 m and a period of 6 s. The

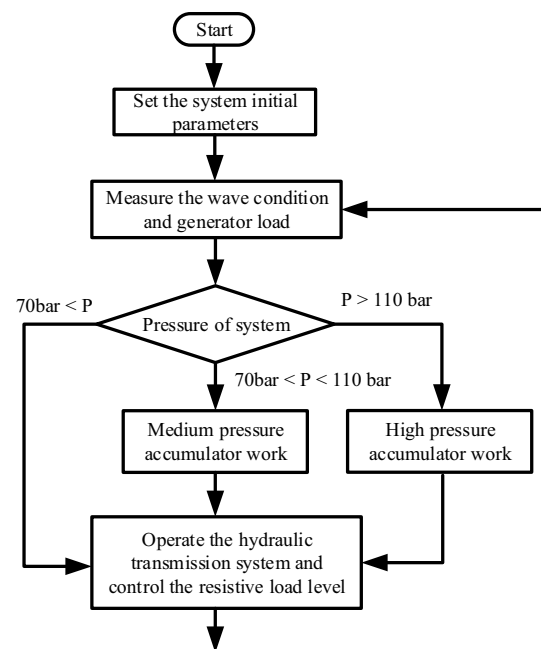


Fig. 7 Proposed control strategy

superiority of charging one accumulator to 110 bar to work in the high input power case is shown in Fig. 9. The system worked under the same condition with two different accumulators pre-charged pressure value [110 bar (HPA) and 70 bar (MPA)]. As can be seen, with the higher accumulator pre-charged pressure, the system can reach a steady state faster. System pressure, flow rate, torque, speed, and output power were smoothed at a constant level for the whole time and the hydraulic motor was working at optimal efficiency value (HPA). While in (MPA), when the 70 bar pre-charged pressure accumulator was used, it took 30 s to charge the pressure to 110 bar to achieve the best working condition. Although the motor efficiency reached maximum value after 20 s, the power loss during that charge time can be significant.

The proposed control strategy was investigated by applying the wave power profile as in Fig. 10 to the hydraulic simulation model. The wave power profile was divided into three stages, the first 60 s is low power, the next 60 s is high power and the last 60 s is medium power. The system performance which was controlled by the proposed strategy was compared to that with the load was controlled at a fixed medium value. Figure 10 shows the simulation results when the fixed load value was applied as a conventional case. As can be seen, during the low input power stage, the load at a medium level was still larger than the input potential that caused the high force acting on the buoy. This force prevented the buoy motion that reduced the displacement a lot. The output power was only 1 kW with the efficiency was about 0.68. The

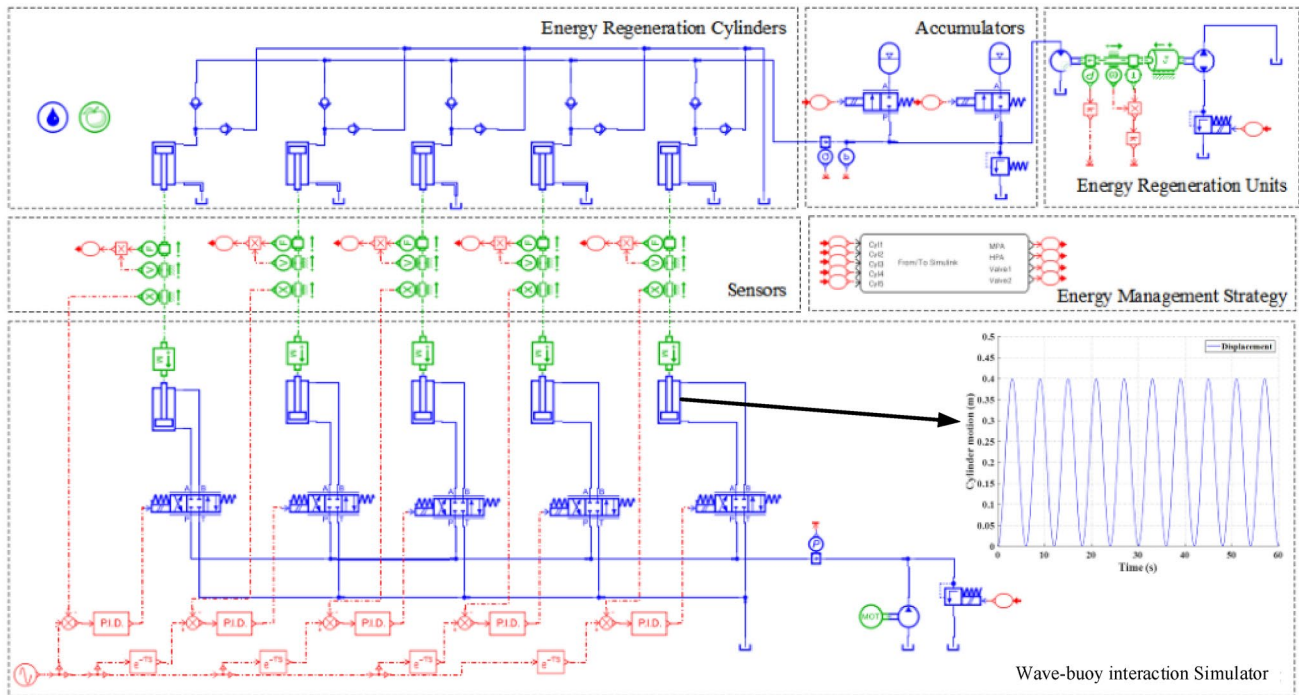


Fig. 8 WEC system AMESIM hydraulic model

remaining time, the system only worked at a medium potential since the medium load cannot increase the system pressure. Although the motor efficiency can reach to the optimal value, the output power was not high since the system cannot absorb all potential input power. The output power was 2.6 kW when the absorbed wave power was only 3 kW for the remaining time. Figure 10 also shows system performance when the proposed control strategy was applied. The system load was controlled based on the input power then the system worked at the optimal condition in all stages of wave power. Thanks to accumulator switching, the system can easily achieve a stable state that can improve motor efficiency. Output power was about 1.5 kW in case of low input power, 4 kW in case of high input power and 2.6 kW in case of medium input power. All cases had an efficiency higher than 0.8, and in the case of high and medium input power, the system worked at the highest efficiency range. These results from Figs. 9 and 10 show the effectiveness of the proposed control

strategy. The system performance was improved and the best working condition was achieved.

The proposed control strategy was also verified by the experiment. Figure 11 shows the experimental results of the hydraulic test rig under the same input conditions of the simulation test. Although there was a small decrease in the output power due to some frictions, the losses that were not included in the simulation model, the results express that the system was working at a very high performance similar to the simulation results. The motor efficiency was always kept at the optimal range.

5 Conclusions

This paper presented an experimental investigation on the WEC using hydraulic PTO. The description of the main parts and working principle, mathematical model,

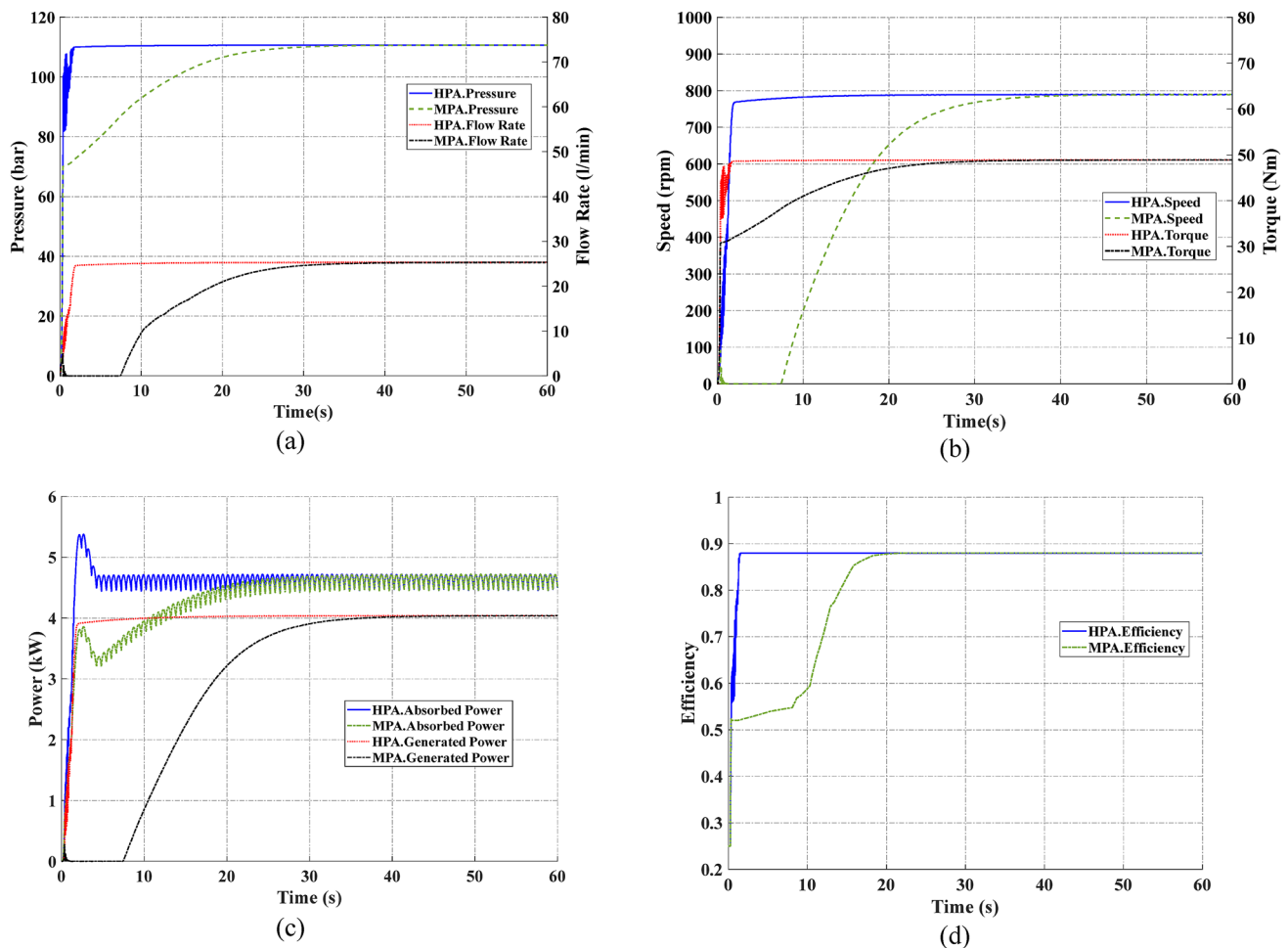


Fig. 9 Simulation results for the cases of high input power, high load with two different accumulators pre-charged pressure (HPA 110 bar, MPA 70 bar)

simulation and experiments were carried out. The hydraulic motor has a major impact on the overall efficiency of the transmission. By adding more accumulators and independently activating them, the motor and hydraulic system can reach a steady state faster which helps reducing loss due to lag time. The control strategy was proposed to maximize the efficiency by selecting the optimal combination of the accumulator pre-charged pressure and load condition to meet a certain wave input power. The simulation had been done to investigate the performance of the

system and compare it with that of the experiment. Good agreement between experimental and simulation results validated the improvement in efficiency using the proposed strategy. During the low input power stage, the proposed strategy can achieve 1.5 kW output power with 80% efficiency while the conventional strategy only achieves 1 kW output power and 68% efficiency. And during the high input power case, the proposed strategy can generate 4 kW output power while only 2.6 kW can be generated by the conventional strategy. Future works will focus on the variable hydraulic motor. In this type, maximize routine can be achieved by selecting the optimal combination of resistive load and displacement of the motor to meet the working condition demand.

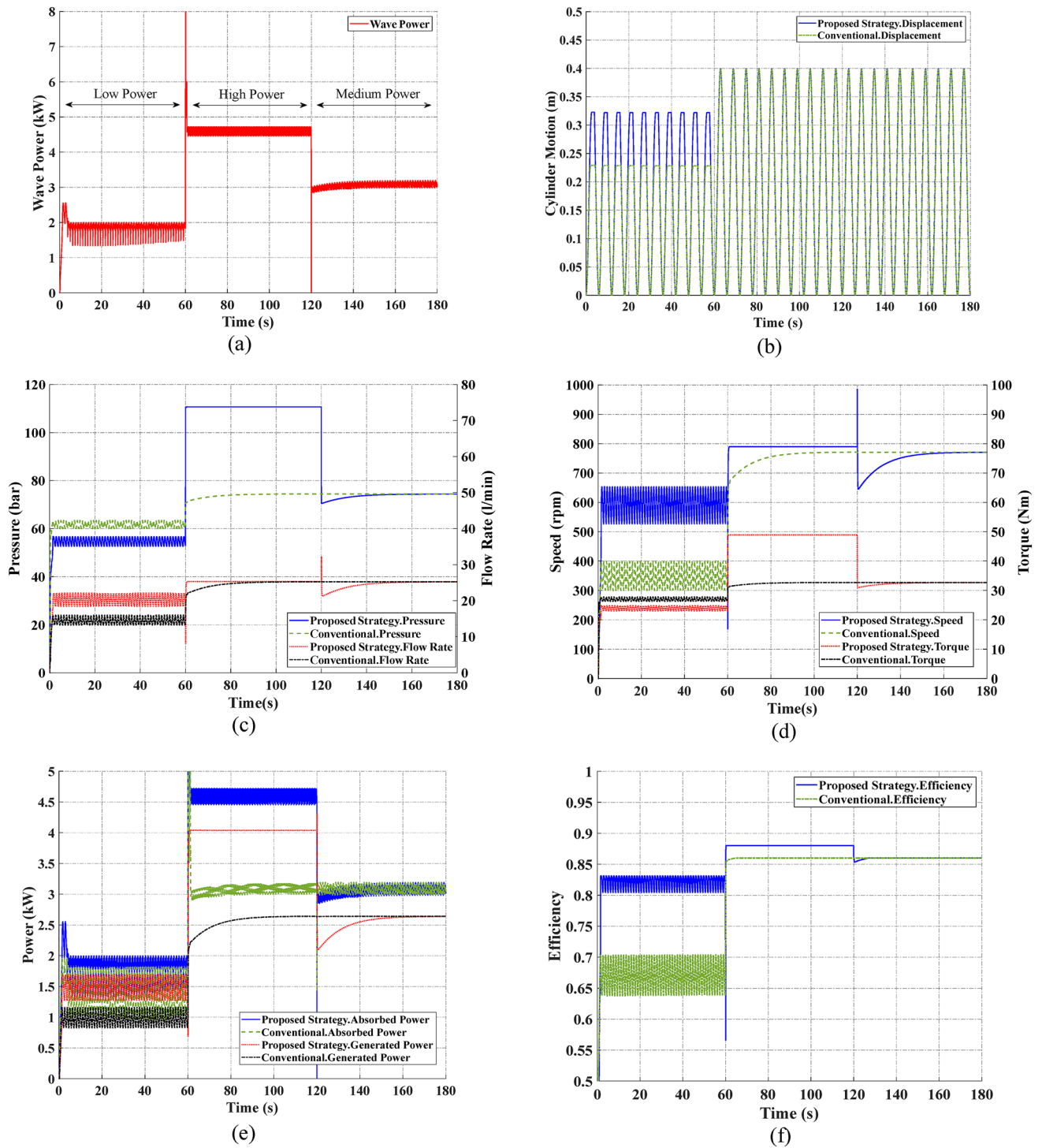


Fig. 10 Simulation results of system performance using the conventional strategy and the proposed control strategy

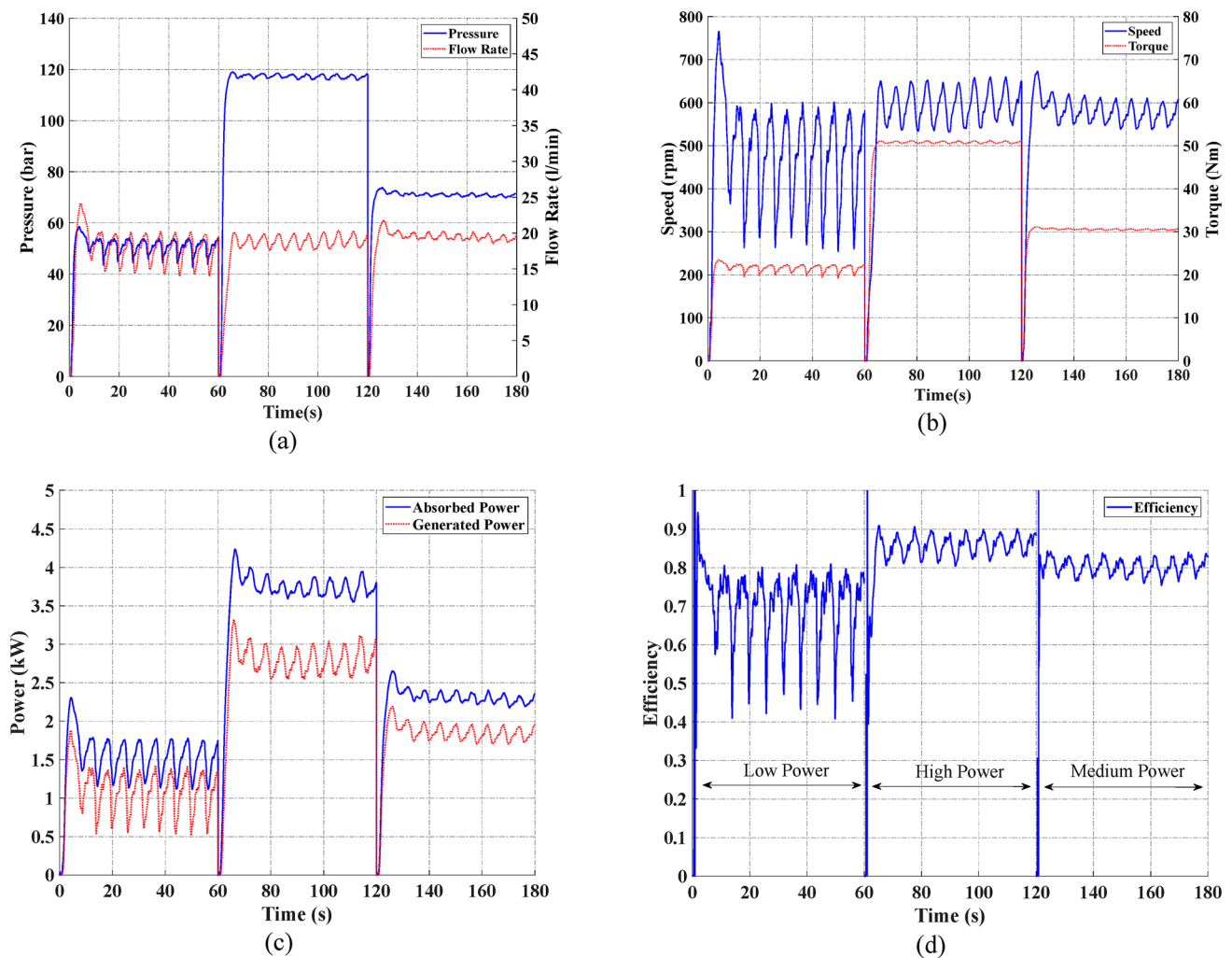


Fig. 11 Experimental results of system performance using the proposed control strategy

Acknowledgements This research was supported by Basic Science Research Program through the National Research Foundation of Korea (NRF) funded by the Ministry of Science and ICT, South Korea (NRF-2020R1A2B5B03001480).

References

- Johannes, F. (2007). A review of wave-energy extraction. *Marine Structures*, 20, 185–201.
- Drew, B., Plummer, A. R., & Sahinkaya, M. N. (2009). A review of wave energy converter technology. *Proceedings of the Institution of Mechanical Engineers, Part A: Journal of Power and Energy*, 223, 887–902.
- Falcão, A. F. O. (2010). Wave energy utilization: A review of the technologies. *Renewable and Sustainable Energy Reviews*, 14, 899–918.
- Iraide, L., Jon, A., Salvador, C., de Iñigo Martínez, A., & Iñigo, K. (2013). Review of wave energy technologies and the necessary power-equipment. *Renewable and Sustainable Energy Reviews*, 27, 413–434.
- Silvia, B., Adrià Moreno, M., Alessandro, A., Giuseppe, P., & Renata, A. (2013). Modeling of a point absorber for energy conversion in Italian seas. *Energies*, 6, 3033–3051.
- Jusoh, M. A., Ibrahim, M. Z., Daud, M. Z., Albani, A., & Yusop, Z. M. (2019). Hydraulic power take-off concepts for wave energy conversion system: A review. *Energies*, 12, 4510.
- Binh, P. C., Tri, N. M., Dung, D. T., Ahn, K. K., Kim, S. J., & Koo, W. (2016). Analysis, design and experiment investigation of a novel wave energy converter. *IET Generation, Transmission and Distribution*, 10, 460–469.
- Dang, T. D., Nguyen, M. T., Phan, C. B., & Ahn, K. K. (2019). Development of a wave energy converter with mechanical power take-off via supplementary inertia control. *International Journal of Precision Engineering and Manufacturing-Green Technology*, 6, 497–509.
- Dang, T. D., Phan, C. B., & Ahn, K. K. (2019). Design and Investigation of a novel point absorber on performance optimization mechanism for wave energy converter in heave mode.

- International Journal of Precision Engineering and Manufacturing-Green Technology*, 6, 477–488.
10. Dang, T. D., Phan, C. B., & Ahn, K. K. (2019). Modeling and experimental investigation on performance of a wave energy converter with mechanical power take-off. *International Journal of Precision Engineering and Manufacturing-Green Technology*, 6, 751–768.
 11. Tri, N. M., Binh, P. C., & Ahn, K. K. (2018). Power take-off system based on continuously variable transmission configuration for wave energy converter. *International Journal of Precision Engineering and Manufacturing-Green Technology*, 5, 89–101.
 12. Ocean power technologies. <https://www.oceanpowertechnologies.com>. Accessed 2015.
 13. Wave Star Energy. <https://www.wavestarenergy.com>. Accessed 2015
 14. Choi, K. S., Yang, D. S., Park, S. Y., & Cho, B. H. (2012). Design and performance test of hydraulic PTO for wave energy converter. *International Journal of Precision Engineering and Manufacturing*, 13(5), 795–801.
 15. Falcão, A. F. O. (2017). Modeling and control of oscillating-body wave energy converters with hydraulic power take-off and gas accumulator. *Ocean Engineering*, 34, 2021–2032.
 16. Ricci, P., Lopez, J., Santos, M., Ruiz-Minguela, P., Villate, J. L., Salcedo, F., et al. (2011). Control strategies for a wave energy converter connected to a hydraulic power takeoff. *IET Renew Power Generation*, 5, 234–244.
 17. Joseba, L., Juan, C. A., Carlos, A., Patxi, E., Maider, S., & Pierpaolo, R. (2012). Design, construction and testing of a hydraulic power take-off for wave energy converters. *Energies*, 5, 2030–2052.
 18. Do, H. T., Dinh, Q. T., Nguyen, M. T., Phan, C. B., Dang, T. D., et al. (2015). Effects of non-vertical linear motions of a hemispherical float wave energy converter. *Ocean Engineering*, 109, 430–438.
 19. Do, H. T., Dinh, Q. T., Nguyen, M. T., Phan, C. B., Dang, T. D., et al. (2017). Proposition and experiment of a sliding angle self-tuning wave energy converter. *Ocean Engineering*, 132, 1–10.
 20. Tri, N. M., Truong, D. Q., Binh, P. C., Dung, D. T., Lee, S., et al. (2016). A Novel control method to maximize the energy-harvesting capability of an adjustable slope angle wave energy converter. *Renewable Energy*, 97, 518–531.
 21. Do, H. T., Dang, T. D., & Ahn, K. K. (2018). A multi-point-absorber wave-energy converter for the stabilization of output power. *Ocean Engineering*, 161, 337–349.
 22. Ahn, K. K., Truong, D. Q., Tien, H. H., & Yoon, J. I. (2012). An innovative design of wave energy converter. *Renewable Energy*, 42, 186–194.
 23. Truong, D. Q., & Ahn, K. K. (2014). Development of a novel point absorber in heave for wave energy conversion. *Renewable Energy*, 65, 183–191.
 24. Cargo, C. J., Hillis, A. J., & Plummer, A. R. (2014). Optimisation and control of a hydraulic power take-off unit for a wave energy converter in irregular waves. *Proceedings of the Institution of Mechanical Engineers, Part A: Journal of Power and Energy*, 228, 462–479.
 25. Cargo, C. J., Plummer, A. R., Hillis, A. J., & Schlotter, M. (2012). Determination of optimal parameters for a hydraulic power take-off unit of a wave energy converter in regular waves. *Proceedings of the Institution of Mechanical Engineers, Part A: Journal of Power and Energy*, 226, 98–111.
 26. Cargo, C. J., Hillis, A. J., & Plummer, A. R. (2016). Strategies for active tuning of Wave Energy Converter hydraulic power take-off mechanisms. *Renewable Energy*, 94, 32–47.
 27. Truong, D. Q., & Ahn, K. K. (2012). Wave prediction based on a modified grey model MGM(1,1) for real-time control of wave energy converters in irregular waves. *Renewable Energy*, 43, 242–255.
 28. Falnes, J. (2002). *Ocean waves and oscillating systems, linear interaction including wave-energy extraction*. Cambridge: Cambridge University.
 29. [Online] WAMIT, Inc version 7.0 user manual. (2015)https://www.wamit.com/manualupdate/history/V70_manual_old.pdf. Accessed 2015

Publisher's Note Springer Nature remains neutral with regard to jurisdictional claims in published maps and institutional affiliations.



Tri-Dung Dang received his B.S. degree in Mechatronics from Ho Chi Minh city University of Technology and Education, Viet Nam in 2013 and Ph.D. from University of Ulsan, Korea in 2019. He is currently working as postdoc researcher in Mechanical Department in University of Ulsan, Korea and Mechatronics Department in Ho Chi Minh city University of Technology and Education, Viet Nam. His research interests include energy management system, hydraulic system, PEM fuel cell vehicles, mechanism and control design for wave energy converter and wind turbine system.



Tri-Cuong Do received the B.S. degree in School of Transportation Engineering from Ha Noi University of Science and Technology, Vietnam in 2017, the M. Sc. degree in School of Mechanical Engineering from University of Ulsan, Korea in 2019. Currently, he is working toward the Ph.D. degrees at the School of Mechanical Engineering, University of Ulsan, South Korea. His research interests include energy regeneration system, hydraulic construction machine, renewable energy, and linear

control theory.



Kyoung Kwan Ahn received the B.S. degree in the Department of Mechanical Engineering from Seoul National University in 1990, the M. Sc. degree in Mechanical Engineering from Korea Advanced Institute of Science and Technology (KAIST) in 1992 and the Ph.D. degree from Tokyo Institute of Technology in 1999, respectively.

Since 2000, he has been with the School of Mechanical Engineering, University of Ulsan, where he is currently a Professor and the Director of the Fluid

Power Control and Machine Intelligence Laboratory.

His main research interests include fluid based triboelectric nano generator, modeling and control of fluid power system, energy saving construction machine, hydraulic robot, and power transmission in the ocean energy. He is the author or coauthor of over 190 SCI(E) papers and 4 books in these areas.

Dr. Ahn serves as an editor of International Journal of Control, Automation and Systems and editorial board of renewable energy, Korean fluid power and construction machine, actuators and so on.